

LOW TEMPERATURE SYNTHESIS AND CHARACTERISATION OF NESQUEHONITE

J. THEO KLOPROGGE¹, WAYDE N. MARTENS¹, LUKE NOTHDURFT²,
LOC V. DUONG³ and GREGORY E. WEBB²

¹ Centre for Instrumental and Developmental Chemistry, Queensland University of Technology, GPO Box 2434, Brisbane, Q 4001, Australia

E-mail: t.kloprogge@qut.edu.au

² School of Natural Resource Sciences, Queensland University of Technology, GPO Box 2434, Brisbane, Q 4001, Australia,

³ Analytical Electron Microscopy Facility, Queensland University of Technology, GPO Box 2434, Q 4001, Australia

Published as:

Kloprogge, J.T., Martens, W.N., Nothdurft, L., Duong, L.V. and Webb, G.E. (2003) Low temperature synthesis and characterization of nesquehonite. *Journal of Materials Science Letters*, 22(11), 825-829.

Copyright 2003 Springer

<http://www.springerlink.com/openurl.asp?genre=journal&eissn=1573-4811>

Nesquehonite, $\text{Mg}(\text{HCO}_3)(\text{OH})\cdot 2\text{H}_2\text{O}$ or $\text{MgCO}_3\cdot 3\text{H}_2\text{O}$, was named after its type locality in Nesquehoning, Pennsylvania, USA. The structure of nesquehonite can be envisaged as infinite chains of corner sharing MgO_6 octahedra along the *b*-axis. Within these chains CO_3^{2-} groups link 3 MgO_6 octahedra by two common corners and one edge. This structural arrangement causes strong distortion of the octahedra. Chains are interconnected by hydrogen bonds only, whereby each Mg atom is coordinated to two water ligands and one free water molecule is located in between the chains [1, 2].

Under natural conditions nesquehonite can form in evaporites depending on the availability of Mg^{2+} ions in solution relative to other cations, such as Ca^{2+} [3-5]. Additionally, nesquehonite occurs as an alteration product in the form of scales or efflorescences on existing carbonate rocks, serpentine, or volcanic breccias [6-11]. Interestingly it has also been observed on the surface of a limited number of meteorites found in Antarctic regions, where it has formed by reactions of the meteorite minerals with terrestrial water and CO_2 at near freezing temperatures [12-16]. Nesquehonite has also been identified on the surfaces of manmade materials, such as bricks and mortar [17, 18].

The synthesis of nesquehonite forms a continuation of our work on the synthesis and study of the vibrational spectroscopy of natural and synthetic minerals in the hydroxide (brucite, gibbsite, boehmite, etc.) [19-23], carbonate (cerussite, azurite, malachite, etc.) [24-26] and hydroxycarbonate (hydrotalcite) [21, 27-32] groups. This work aims at describing a simple method for the synthesis of nesquehonite and the detailed characterization of the structure and morphology by X-

ray diffraction (XRD), vibrational spectroscopy and scanning electron microscopy (SEM).

The first nesquehonite sample was synthesized by adding the stoichiometric amounts of Na_2CO_3 and $\text{MgCl}_2 \cdot 6\text{H}_2\text{O}$ into deionised water and shaking the solution for ~ 10 seconds. The solution containing the precipitate was then allowed to stand for 1 hour, after which the precipitate was filtered, washed with deionised water and dried in air. The second nesquehonite sample was synthesized by adding a solution of 4.9 g Na_2CO_3 in 67 ml H_2O to 8.13 g $\text{MgCl}_2 \cdot 6\text{H}_2\text{O}$ in 450 ml H_2O over a period of 5 minutes and then stirring for another 5 minutes. The resulting precipitate was allowed to stand and settle for 5 days. The precipitate was washed with deionised water until clear of chloride anions and was then allowed to dry overnight at 50°C . Table 1 gives an overview of the synthesis conditions applied and the resulting products.

The crystalline material was characterised using powder XRD. The XRD analyses were carried out on a Philips wide-angle PW 1050/25 vertical goniometer applying $\text{CuK}\alpha$ radiation. The sample was measured at 50 % RH in stepscan mode with steps of $0.02^\circ 2\theta$ and a scan speed of 1.00° per minute from 2 to $75^\circ 2\theta$. Images were obtained on a FEI QUANTA 200 Environmental Scanning Electron Microscope operating at high vacuum and 15 kV. Infrared absorption (IR) spectra were recorded in triplicate by accumulating 64 scans at 4 cm^{-1} resolution between 400 cm^{-1} and 4000 cm^{-1} for each sample using a Perkin-Elmer 1600 series Fourier transform infrared spectrometer equipped with a LITA detector. To obtain the Raman spectrum the sample was placed on a polished metal surface on the stage of an Olympus BHSM microscope, which is equipped with 10x, 20x, and 50x objectives. The microscope is part of a Renishaw 1000 Raman microscope system, which also includes a monochromator, a filter system and a CCD detector (1024 pixels). The Raman spectra were excited by a Spectra-Physics model 127 He-Ne laser producing highly polarised light at 633 nm and collected at a resolution of 2 cm^{-1} and a precision of $\pm 1 \text{ cm}^{-1}$ in the range between 200 and 4000 cm^{-1} . Repeated acquisition on the crystals using the highest magnification (50x) were accumulated to improve the signal to noise ratio in the spectra. Spectra were calibrated using the 520.5 cm^{-1} line of a silicon wafer. Baseline adjustment, smoothing and normalisation were performed using the Spectralcalc software package GRAMS (Galactic Industries Corporation, NH, U.S.A.). Band component analysis was carried out using the peakfit software package by Jandel Scientific. Lorentz-Gauss cross product functions were used throughout and peakfitting was carried out until squared correlation coefficients with $r^2 > 0.995$ were obtained.

Both nesquehonite samples formed as white powders. Under the optical microscope they exhibit a transparent to translucent diaphaneity and vitreous luster. Fig. 1 shows the XRD patterns of the two samples. The first sample formed during shaking of the solution for a short period of time exhibits very low crystallinity compared to the second sample. In addition it contains a small amount of an unidentifiable phase not present in the second sample. The pattern is in complete agreement with the pattern present in the JCPDS database under card 70-1433. Table 2 gives an overview of the observed basal spacings and intensities in comparison to the JCPDS card 70-1433 for the 15 strongest lines. The crystal structure of nesquehonite has been refined and published in several papers [1, 2]. It is monoclinic with spacegroup $\text{P}21/\text{n}$, $Z = 4$ and unit cell parameters of $a = 7.705 \text{ \AA}$, $b = 5.367 \text{ \AA}$, $c = 12.121 \text{ \AA}$ and $\beta = 90^\circ.45'$ as reported by Stephan and MacGillavry [2] or $a = 7.701 \text{ \AA}$, $b = 5.365 \text{ \AA}$, $c = 12.126 \text{ \AA}$ and $\beta = 90^\circ.41'$ as reported by Giester et al. [1]. Our

powder diffraction patterns of the two nesquehonite samples agree well with these results.

The morphology of the two samples is significantly different. Sample 1 shows a conglomerate of very thin platelets with a diameter smaller than 2 μm (Fig. 2a), whereas sample 2 shows well-formed needles up to 100 μm in length and about 5 μm in diameter (Fig 2b). EDX analysis confirms that the needles are pure nesquehonite (Fig. 2c).

The IR and Raman spectra of sample 2 are displayed in Fig. 3. Where CO_3^{2-} is present as a free ion it exhibits a space group of D_{3h} . As a result the bending non-planar mode $\nu_2(A''_2)$, the antisymmetrical stretching mode $\nu_3(E')$, and the bending angular mode $\nu_4(E')$, occur in the IR spectrum at 880, 1415 and 680 cm^{-1} , whereas the symmetric stretching mode $\nu_1(A'_1)$ is IR inactive. The $\nu_1(A'_1)$, $\nu_3(E')$ and $\nu_4(E')$ occur in the Raman spectra[33, 34]. In comparison to free CO_3^{2-} a shift towards lower wavenumbers is generally observed in minerals. The IR spectrum of nesquehonite displays ν_2 around 851 cm^{-1} . Two strong bands occur around 1466 and 1512 cm^{-1} . In addition a shoulder is present at 1510 cm^{-1} . The 1645 cm^{-1} band can be ascribed to an OH-bending mode of water, resulting from the presence of a small amount of adsorbed water on the surfaces of the nesquehonite crystals. The three bands around 1466, 1510 and 1512 cm^{-1} are ascribed to the split ν_3 . The carbonate ν_4 mode is visible in both the IR and Raman spectra. In the IR spectrum a split mode is observed at 698 and 748 cm^{-1} , whereas the accompanying Raman bands are observed at 701 and 768 cm^{-1} . The Raman active ν_1 mode is present as a strong band at 1096 cm^{-1} . Some IR inactive modes show up as very weak bands, most probably due to stresses in the nesquehonite crystals e.g. at 1418 and 1510 cm^{-1} in the Raman spectrum associated with the ν_3 mode).

The three crystal water molecules can be recognized in the OH-stretching region between 2500 and 4000 cm^{-1} . In both the Raman and IR spectra a very sharp band occurs at 3555 cm^{-1} . This band previously has been reported as being characteristic for nesquehonite, artinite and hydromagnesite [35]. In addition, two broader bands are present in the IR spectrum at 3119 and 3247 cm^{-1} plus a shoulder at 3442 cm^{-1} , which can be ascribed to OH-stretching modes of water in the crystal structure of the nesquehonite. In the Raman spectrum corresponding broad bands are observed at 3135 and 3273 cm^{-1} . The very broad band centered around 3200 cm^{-1} is probably related to adsorbed water.

Acknowledgements

The financial support and infrastructure of the Queensland University of Technology, Centre for Instrumental and Developmental Chemistry is gratefully acknowledged. This work is part of a Queensland University of Technology Small Research Grant.

References

1. G. GIESTER, C. L. LENGAUER and B. RIECK, *Mineralogy and Petrology* **70** (2000) 153.
2. G. W. STEPHAN and C. H. MACGILLAVRY, *Acta Crystallogr., Sect. B* **28** (1972) 1031.
3. D. B. LEVY, J. A. SCHRAMKE, K. J. ESPOSITO, T. A. ERICKSON and J. C. MOORE, *Applied Geochemistry* **14** (1998) 53.
4. R. W. RENAUT, *Hydrobiologia* **197** (1990) 67.

5. M. VANTHOURNHOUT, *Trib. CEBEDEAU (Cent. Belge Etude Doc. Eaux)* **25** (1972) 187.
6. E. C. KIRCHNER and P. SIMONSBERGER, *Karinthin* **87** (1982) 395.
7. R. FISCHBECK and G. MUELLER, *Contrib. Mineral. Petrol.* **33** (1971) 87.
8. R. FISCHBECK, *Neues Jahrb. Mineral., Abh.* **126** (1976) 269.
9. R. BROUSSE and H. GUERIN, *Bull. Soc. Franc., Mineral. Crist.* **89** (1966) 281.
10. R. BROUSSE, A. LAMBERT and F. CHANTRET, *C. R. Congr. Natl. Soc. Savantes, Sect. Sci.* **95** (1975) 207.
11. J. SUZUKI and M. ITO, *Ganseki Kobutsu Kosho Gakkaishi* **69** (1974) 275.
12. M. M. GRADY, E. K. GIBSON, JR., I. P. WRIGHT and C. T. PILLINGER, *Meteoritics* **24** (1989) 1.
13. A. J. T. JULL, S. CHENG, J. L. GOODING and M. A. VELBEL, *Science (Washington, DC, United States)* **242** (1988) 417.
14. M. MIYAMOTO, *Earth and Planetary Science Letters* **96** (1989) 229.
15. M. A. VELBEL, D. T. LONG and J. L. GODDING, *Geochimica et Cosmochimica Acta* **55** (1991) 67.
16. H. YABUKI, A. OKADA and M. SHIMA, *Sci. Pap. Inst. Phys. Chem. Res. (Jpn.)* **70** (1976) 22.
17. I. GROSVALDS, S. LAGZDINA and U. SEDMALIS, *Internationale Baustofftagung, 13th, Weimar, Sept. 24-26, 1997* **2** (1997) 2/0599.
18. M. S. JONES, R. D. WAKEFIELD and G. FORSYTH, *Materiales de Construcción (Madrid)* **49** (1999) 3.
19. R. L. FROST, J. T. KLOPROGGE, S. C. RUSSELL and J. L. SZETU, *Applied Spectroscopy* **53** (1999) 423.
20. R. L. FROST, J. T. KLOPROGEE, S. C. RUSSELL and J. SZETU, *Applied Spectroscopy* **53** (1999).
21. R. L. FROST, J. KLOPROGGE, S. C. RUSSELL and J. L. SZETU, *Thermochim. Acta* **329** (1999) 47.
22. R. L. FROST, J. T. KLOPROGGE, S. C. RUSSELL and J. L. SZETU, *Appl. Spectrosc.* **53** (1999) 423.
23. J. T. KLOPROGGE, H. D. RUAN and R. L. FROST, *Journal of Materials Science* **37** (2002) 1121.
24. Z. DING, R. L. FROST and J. T. KLOPROGGE, *Journal of Materials Science Letters* **21** (2002) 981.
25. R. L. FROST, Z. DING, J. T. KLOPROGGE and W. N. MARTENS, *Thermochimica Acta* **390** (2002) 133.
26. R. L. FROST, W. N. MARTENS, L. RINTOUL, E. MAHMUTAGIC and J. T. KLOPROGGE, *Journal of Raman Spectroscopy* **33** (2002) 252.
27. L. HICKEY, J. T. KLOPROGGE and R. L. FROST, *Journal of Materials Science* **35** (2000) 4347.
28. T. E. JOHNSON, W. MARTENS, R. L. FROST, Z. DING and J. T. KLOPROGGE, *Journal of Raman Spectroscopy* **33** (2002) 604.
29. J. T. KLOPROGGE and R. L. FROST, *J. Solid State Chem.* **146** (1999) 506.
30. J. T. KLOPROGGE, L. HICKEY and R. L. FROST, *Applied Clay Science* **18** (2001) 37.
31. J. T. KLOPROGGE, L. HICKEY and R. L. FROST, *Journal of Materials Science Letters* **21** (2002) 603.
32. J. T. KLOPROGGE, D. WHARTON, L. HICKEY and R. L. FROST, *American Mineralogist* **87** (2002) 623.

33. K. NAKAMOTO, *Infrared and Raman Spectra of Inorganic and Coordination Compounds*, 5th ed., John Wiley & Sons, USA, **1997**.
34. V. FARMER, *The Infrared Spectra of Minerals*, Mineralogical Society, England, **1974**.
35. W. B. WHITE, *Amer. Mineral.* **56** (1971) 46.

Table 1. Synthesis conditions applied for the synthesis of nesquehonite and the resulting products.

Sample	Starting material	Temp.	Reaction conditions	Drying conditions	Crystalline products formed	morphology	Crystal size
1	Na ₂ CO ₃ + MgCl ₂ .6H ₂ O	25°C	Shaking solution for 10 seconds, stand for 1 hour	In air at 25°C	nesquehonite + unidentified phase	Very thin plates in large aggregates	Diameter up to 2 μm, thickness < 0.1 μm
2	Na ₂ CO ₃ + MgCl ₂ .6H ₂ O	25°C	Adding carbonate solution to Mg chloride solution in 5 min, stand for 5 days	In oven overnight at 50°C	nesquehonite	Well crystallized needles	Length up to 100 μm, diameter up to 5 μm

Table 2. Overview of the XRD basal spacings and intensities of the 15 strongest lines of nesquehonite.

d-spacing observed (Å)	Rel. Intensity	d-spacing (Å) JCPDS card 70-1433	Rel. Intensity
6.506	70	6.5253	74
		6.4790	100
3.855	100	3.8522	76
3.589	11	3.5896	15
3.241	7	3.2278	18
3.033	22	3.0303	24
2.986	3	2.9837	6
2.784	6	2.7881	10
2.623	4	2.6199	32
2.510	21	2.5165	7
2.173	5	2.1751	5
2.160	3	2.1589	4
2.021	6	2.0201	7
1.927	20	1.9262	19
1.800	4	1.7988	13
1.649	3	1.6479	5

Figure captions

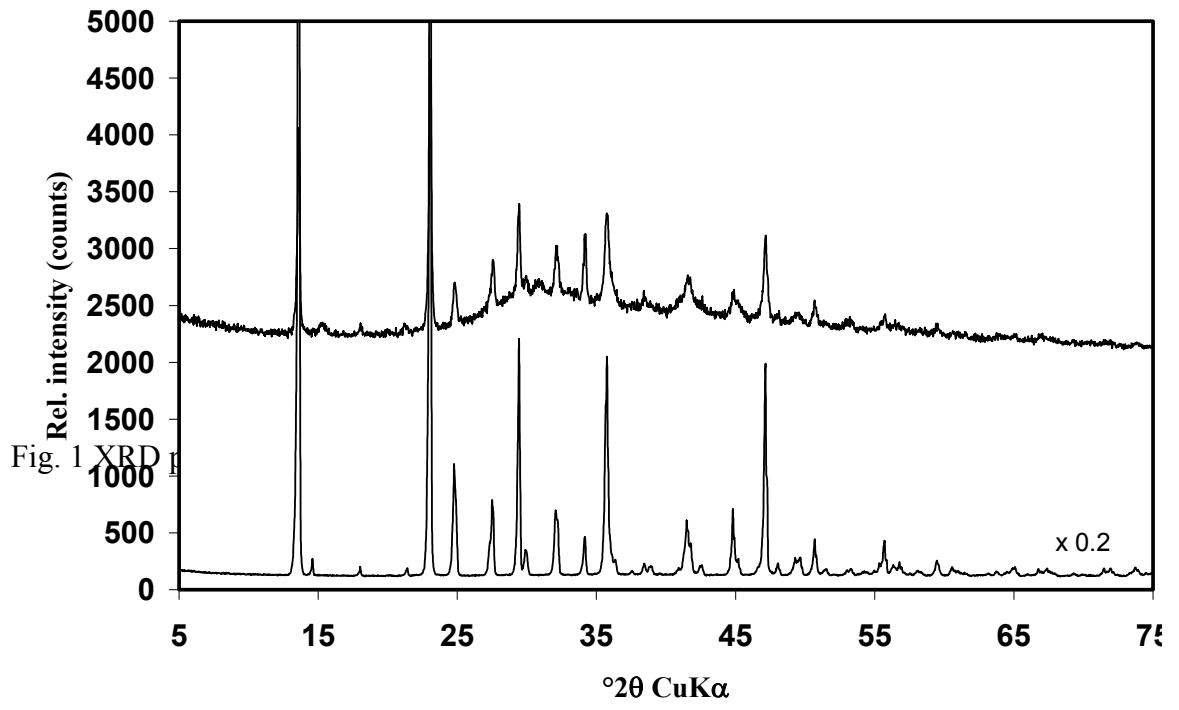
Fig. 1 XRD patterns of synthetic nesquehonite (sample 1 top, sample 2 bottom).

Fig. 2a SEM image of nesquehonite sample 1.

Fig. 2b SEM image of nesquehonite sample 2.

Fig 2c. EDX analysis of nesquehonite sample 2.

Fig. 3 IR and Raman spectra of nesquehonite sample 2 in the range between 500 and 4000 cm^{-1} .



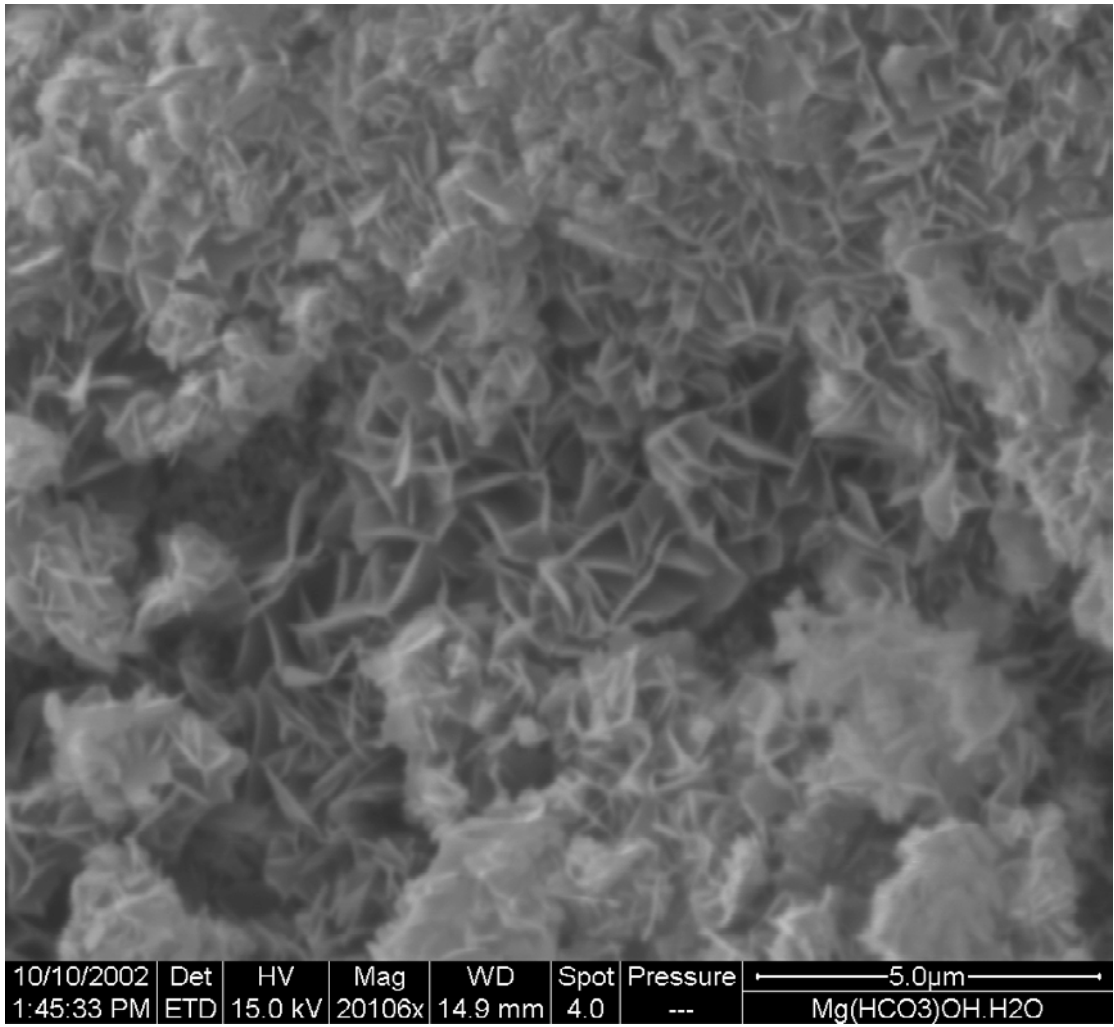


Fig. 2a SEM image of nesquehonite sample 1.

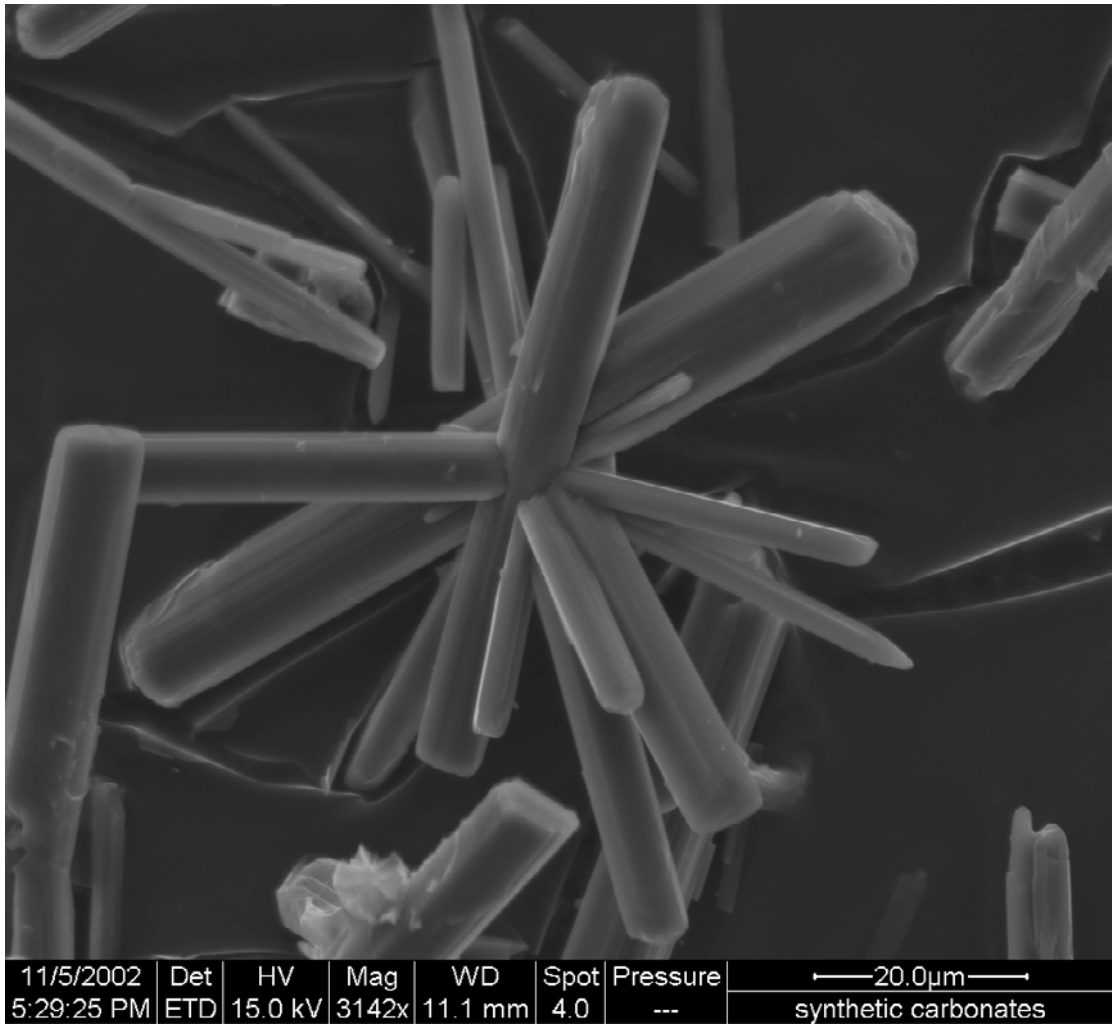


Fig. 2b SEM image of nesquehonite sample 2.

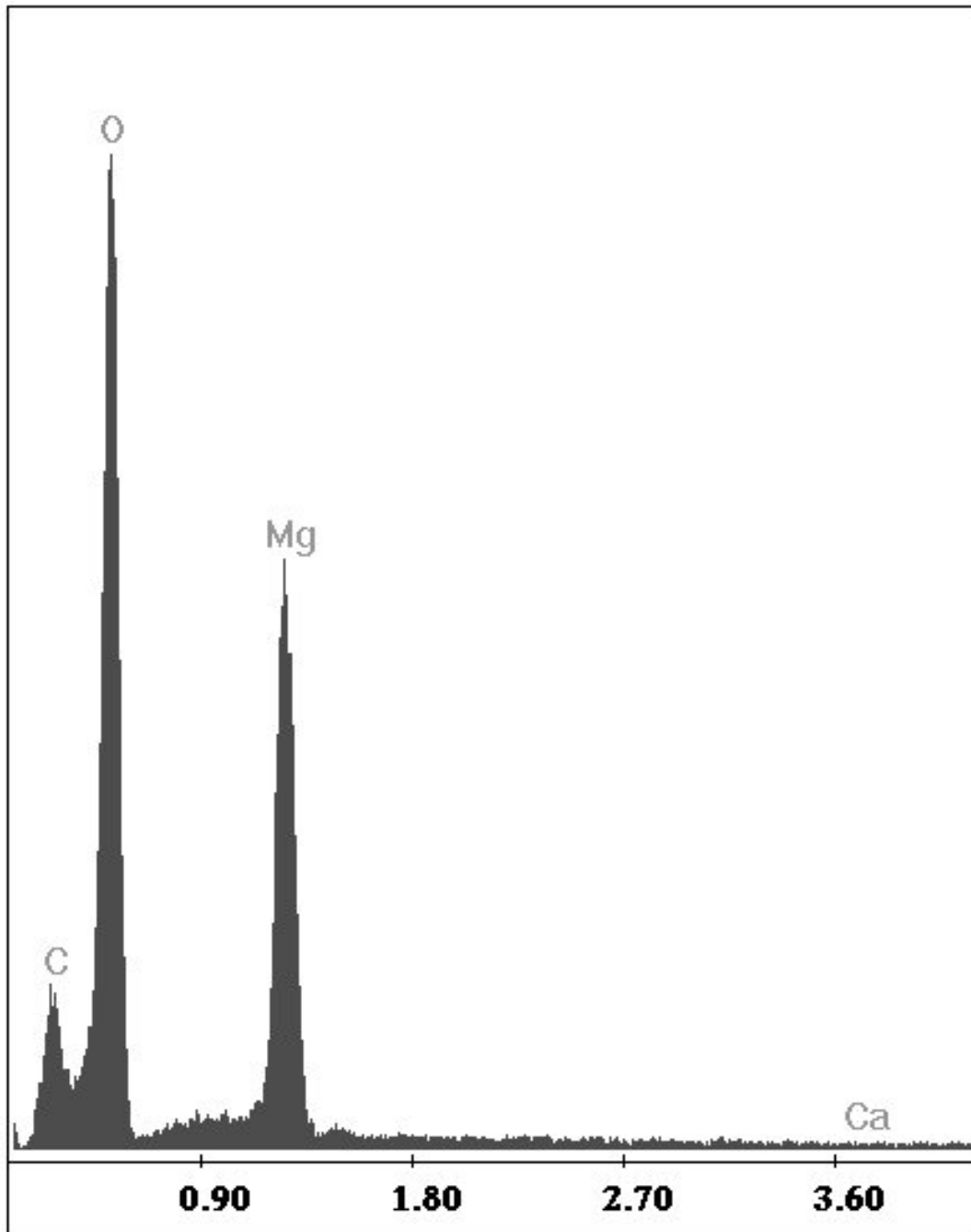


Fig 2c. EDX analysis of nesquehonite sample 2.

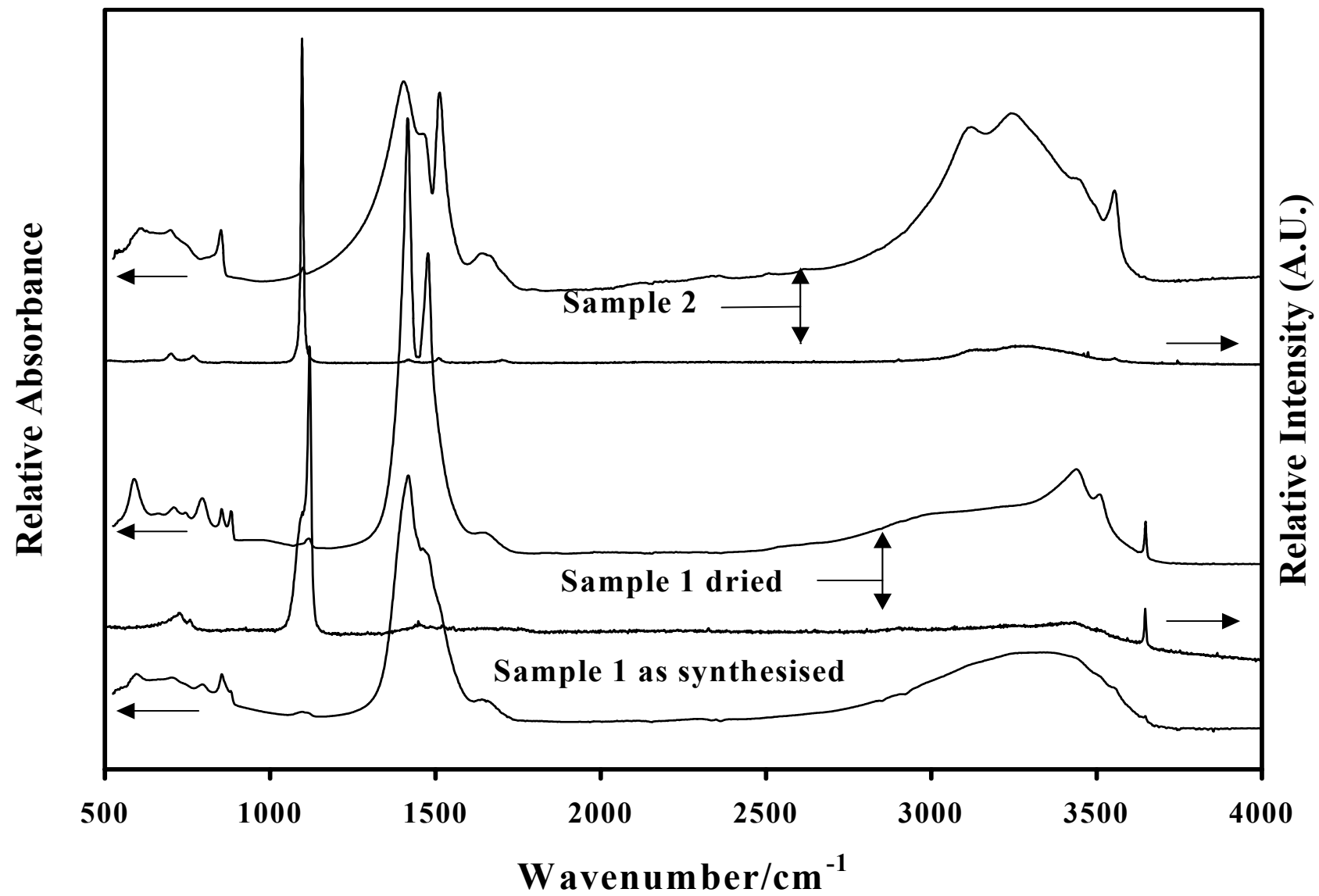


Fig. 3 IR and Raman spectra of nesquehonite in the range between 500 and 4000 cm^{-1} .